Electronic Supplementary Material (ESI) for Nanoscale.

Supporting Information

Rapid Production of Multiple Transition Metal Carbides via Microwave Combustion under Ambient Conditions

Huiyu Jiang, ‡[a] Junfeng Li, ‡[a] Zhiheng Xiao,[b] Bo Wang,[c] Mingzhao Fan,[a] Siqi Xu,[a] and Jun Wan[a,b]*

[a]Hubei Key Laboratory of Biomass Fiber and Ecological Dyeing and Finishing, Wuhan Textile University, Wuhan 430200, Hubei, China.
[b]State Key Laboratory for Hubei New Textile Materials and Advanced Processing Technology, Wuhan Textile University, Wuhan 430200, Hubei, China.
[c]School of Electrical Engineering and Automation, Luoyang Institute of Science and Technology, Luoyang 471023, Henan, China.

‡ These authors contributed equally to the work.
*Correspondence author: wanj@wtu.edu.cn

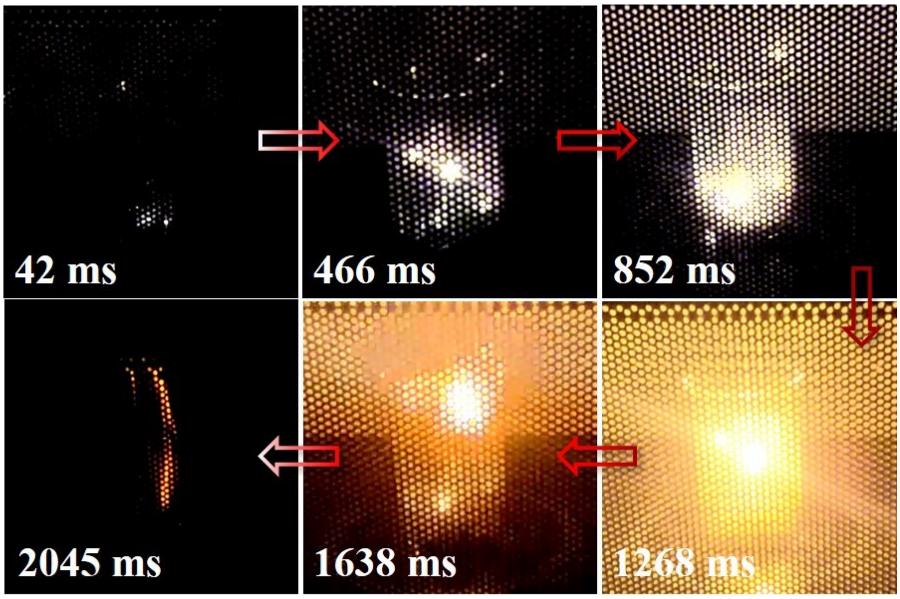

Figure S1. A series of photographs showing the sample during flash ignition with the time interval labeled in two seconds.

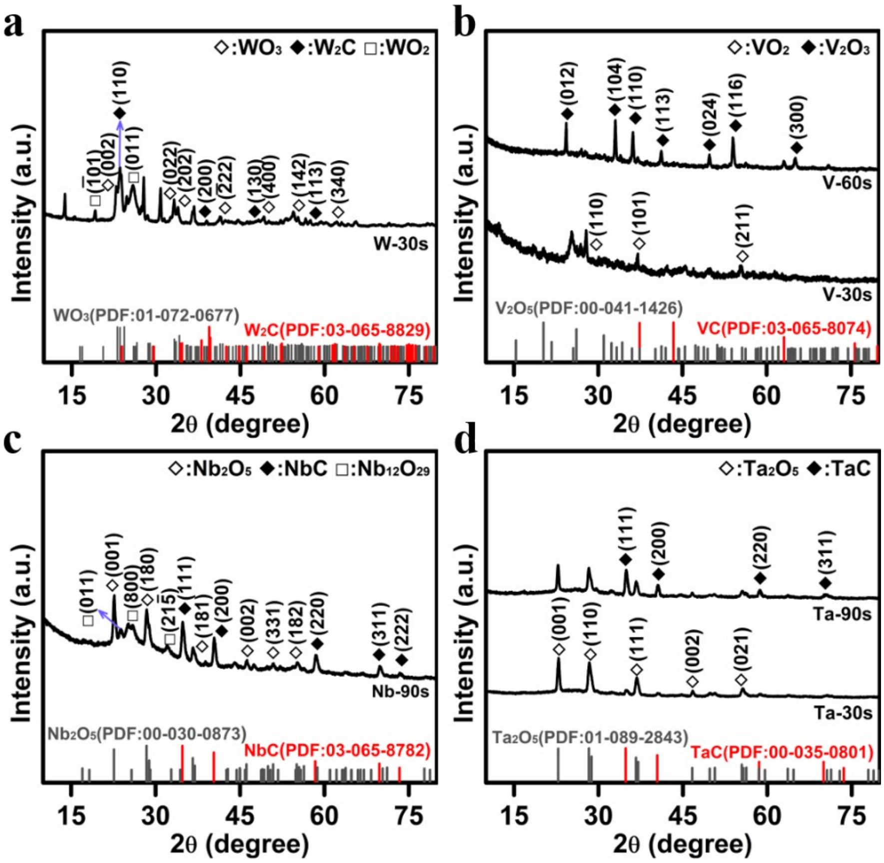

Figure S2. XRD patterns of intermediate reaction condition samples. (a) XRD pattern of the precursor of WO_3/GO composite after microwave treating for 30 s. (b) XRD patterns of V_2O_5/GO composites after microwave treating for 30 s and 60 s. (c) XRD pattern of Nb_2O_5/GO composite after microwave treating for 90 s. (d) XRD patterns of Ta_2O_5/GO composites after microwave treating for 30 s and 90 s.

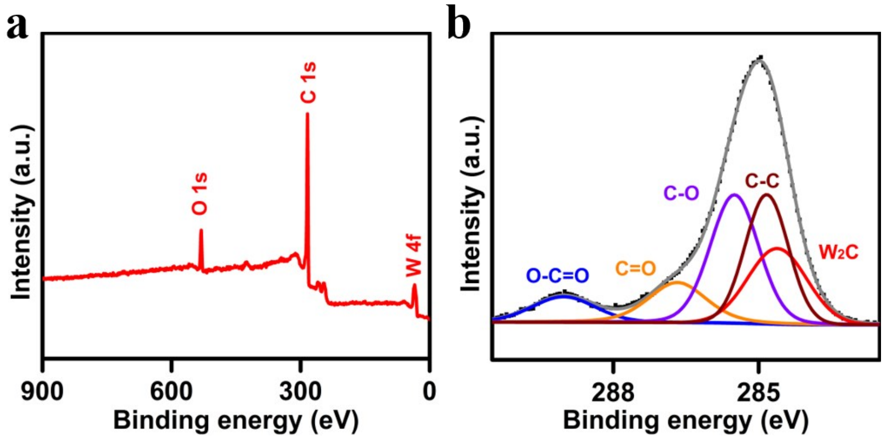

Figure S3. (a) XPS survey spectra and (b) C 1s peaks of the W_2C-90s sample.

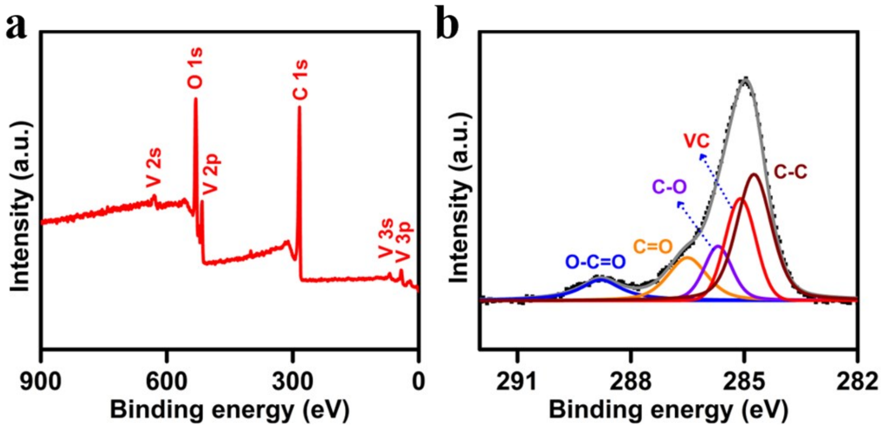

Figure S4. (a) XPS survey spectra and (b) C 1s peaks of the VC-120s sample.

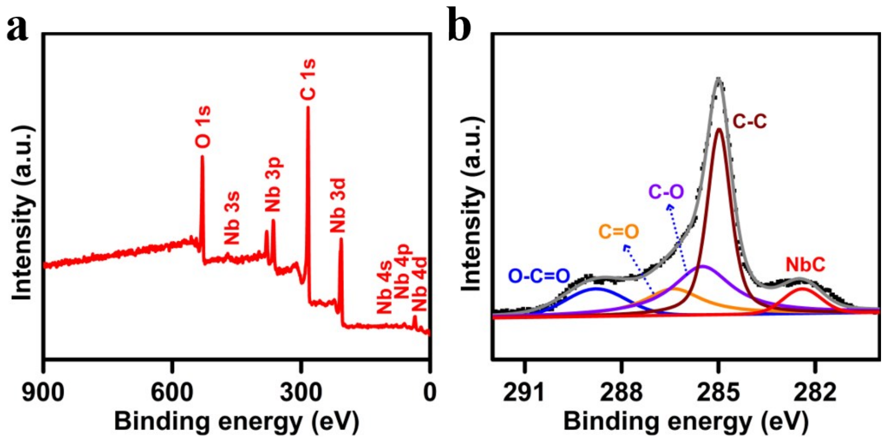

Figure S5. (a) XPS survey spectra and (b) C 1s peaks of the NbC-120s sample.

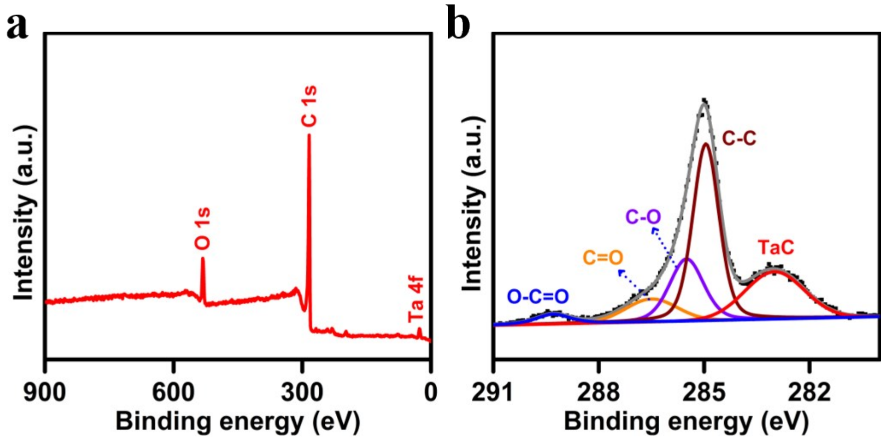

Figure S6. (a) XPS survey spectra and (b) C 1s peaks of the TaC-140s sample.

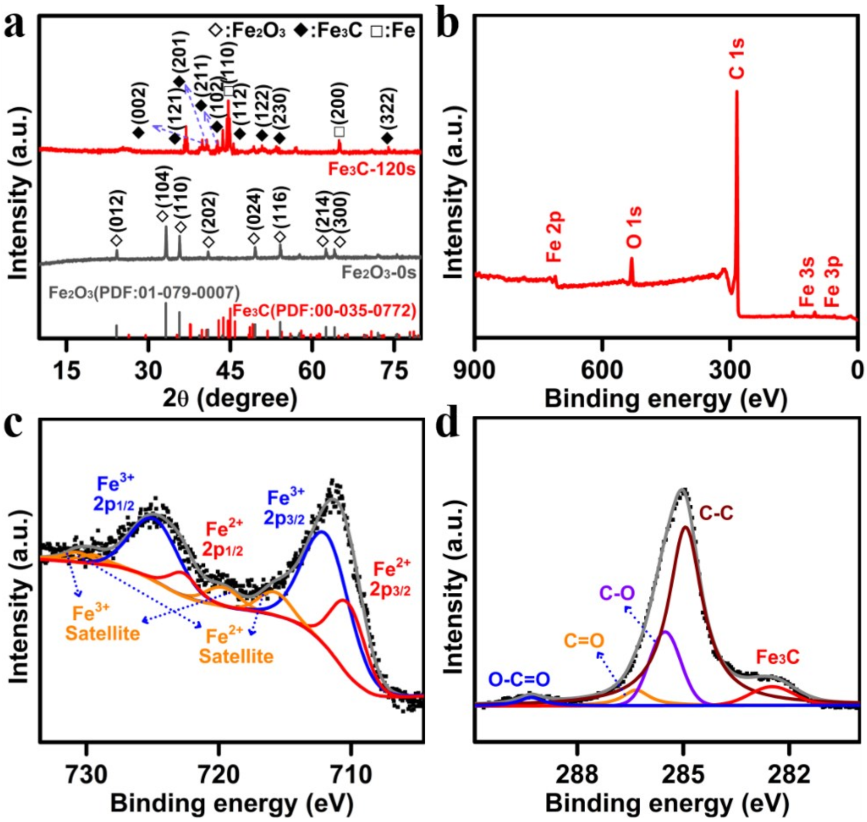

Figure S7. (a) XRD patterns of the pre-synthesis and completed reaction condition samples. (b) XPS survey spectra. (c) Core level Fe 2p XPS spectra and (d) C 1s peaks of the Fe_3C-120s sample.

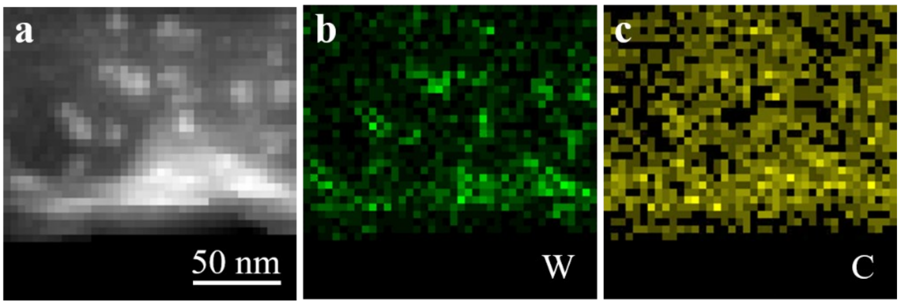

Figure S8. EDS elemental mapping scanning of the W_2C-90s sample from TEM.

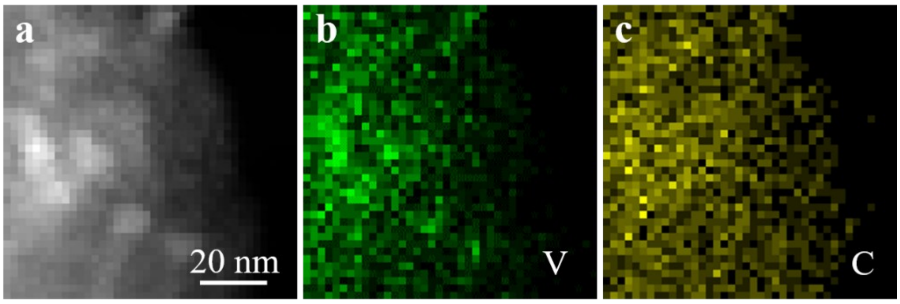

Figure S9. EDS elemental mapping scanning of the VC-120s sample from TEM.

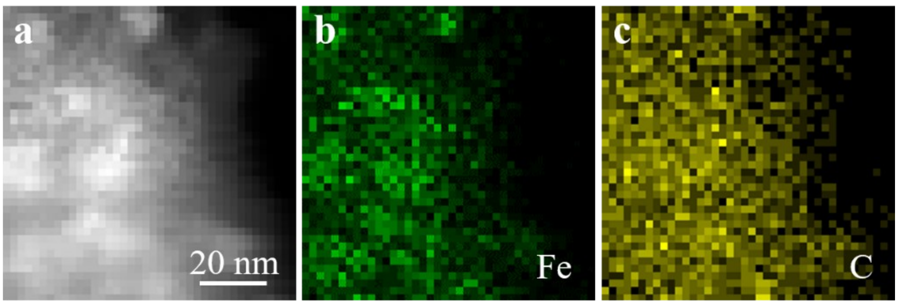

Figure S10. EDS elemental mapping scanning of the Fe_3C-120s sample from TEM.

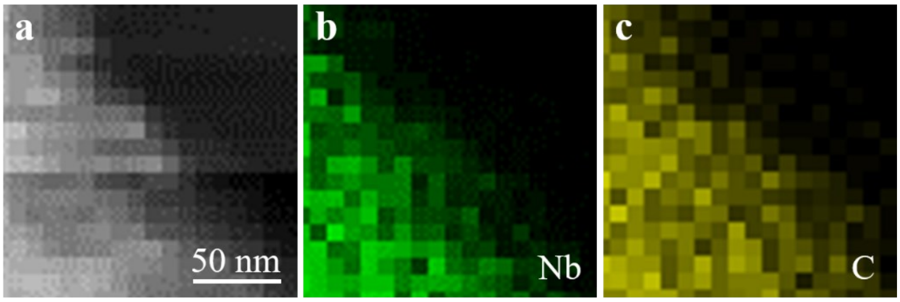

Figure S11. EDS elemental mapping scanning of the NbC-120s sample from TEM.

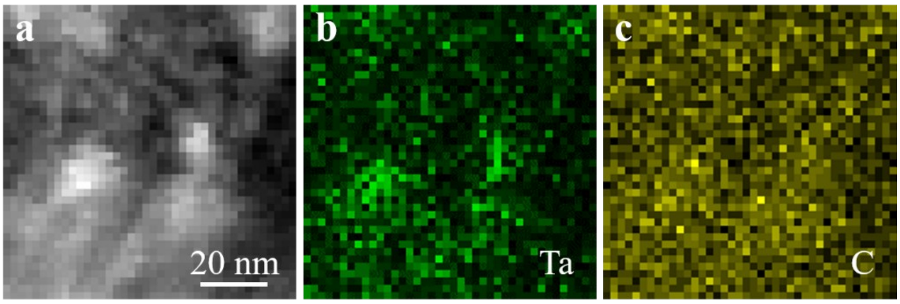

Figure S12. EDS elemental mapping scanning of the TaC-140s sample from TEM.

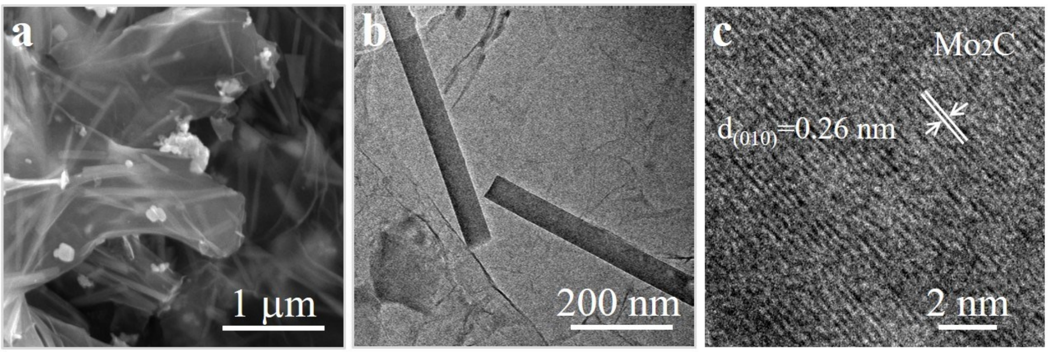

Figure S13. (a) SEM of the MoO3/GO composite. (b,c) TEM and High-resolution images of the Mo2C-120s sample.

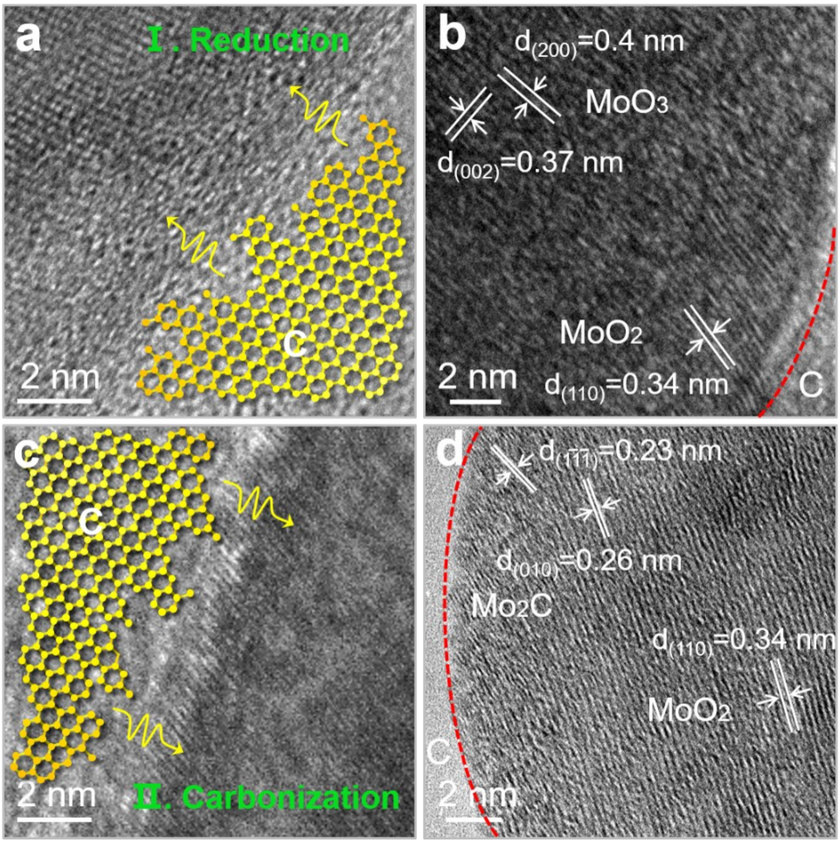

Figure S14. The High-resolution TEM images of the Mo-6s and Mo-100s samples. (a) The reduction process from MoO_3 to MoO_2. (b) The transition boundary of reduction between two crystalline phases. (c) The carbonization process from MoO_2 to Mo_2C. (d) The transition boundary of carbonization between MoO_2 and Mo_2C phases.

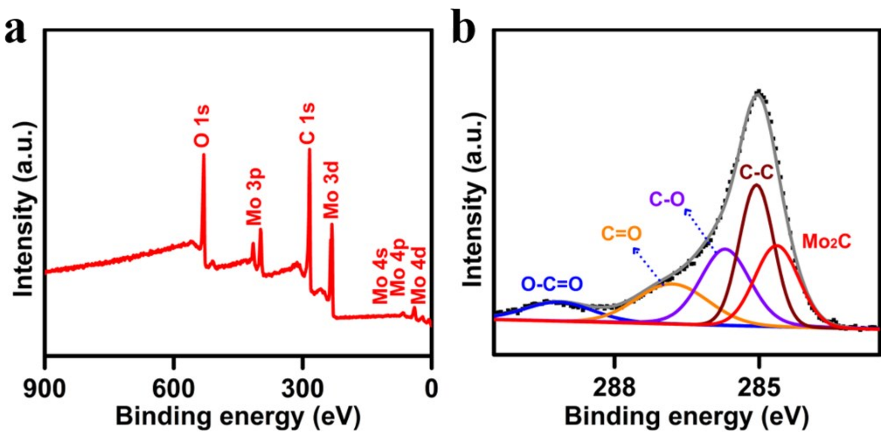

Figure S15. (a) XPS survey spectra and (b) C 1s peaks of the Mo_2C-120s sample.

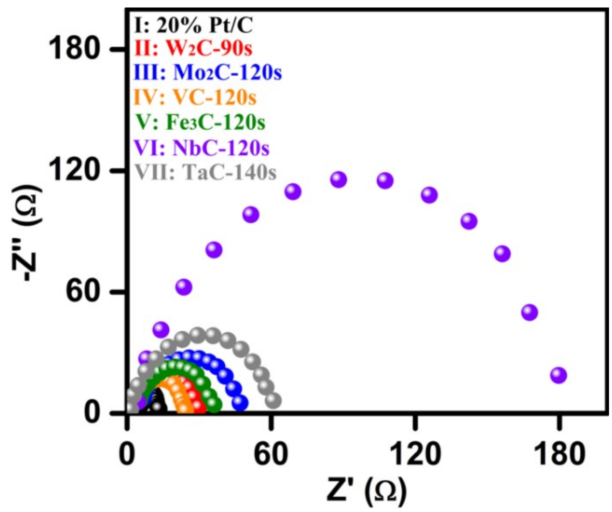

Figure S16. Nyquist plots of the above carbide electrocatalysts.

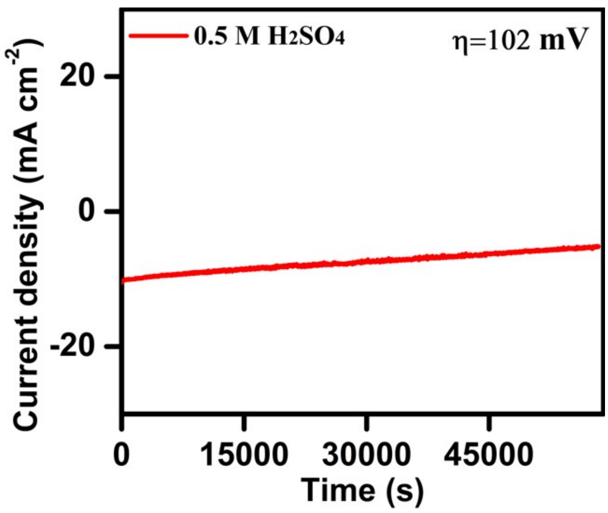

Figure S17. The long-term durability test of VC-120s sample at η=102 mV in 0.5 M H_2SO_4.

Table S1 | Comparison of HER performance in acid media with other electrocatalysts.

Catalyst	Loading (mg cm^{-2})	Electrolyte	Onset potential (mV vs RHE)	Overpotential at 10 mA cm^{-2} (mV vs RHE)	Tafel slope (mV dec^{-1})	Ref.
W_2C/rGO	**0.55**	**0.5 M H_2SO_4**	**38**	**120**	**51**	**This work.**
Mo_2C/rGO	**0.55**	**0.5 M H_2SO_4**	**45**	**138**	**55**	**This work.**
VC/rGO	**0.55**	**0.5 M H_2SO_4**	**21**	**88**	**56**	**This work.**
Fe_3C/rGO	**0.55**	**0.5 M H_2SO_4**	**30**	**116**	**68**	**This work.**
NbC/rGO	**0.55**	**0.5 M H_2SO_4**	**126**	**265**	**112**	**This work.**
TaC/rGO	**0.55**	**0.5 M H_2SO_4**	**48**	**166**	**93**	**This work.**
W_2C/MWNT	0.556	0.5 M H_2SO_4	50	123	45	Nat. Commun. 2016, 7, 13216.
WC NPs	1	0.5 M H_2SO_4	100	125	84	ChemSusChem 2013, 6, 168.
P-W_2C@NC	3.5	0.5 M H_2SO_4	45	89	53	J. Mater. Chem. A 2017, 5, 765.
Fe-WCN	0.4	PH=1 H_2SO_4	~100	220	47.1	Angew. Chem., Int Ed. 2013, 52, 13638.
α-WC/CB	0.724	0.5 M H_2SO_4	<50	260	---	Angew. Chem., Int Ed. 2014, 53, 5131.
WC-CNTs	---	0.05 M H_2SO_4	15	145	72	ACS Nano 2015, 9, 5125.
Porous WC thin film	0.16	0.5 M H_2SO_4	120	274	67	J. Mater. Chem. A 2015, 3, 5798.
Thin film W_2C	---	0.5 M H_2SO_4	---	>300	69	J. Am. Chem. Soc. 2012, 134, 3025.
W_2C microspheres	---	1 M H_2SO_4	50	~170	118	Int. J. Hydrogen. Energ 2008, 33, 6865.
Co_6W_6C	0.28	0.5 M H_2SO_4	26	200	75	Nanoscale 2015, 7, 3130.
Mo_2C@NPC/NPRGO	0.14	0.5 M H_2SO_4	0	34	33.6	Nat Commun. 2016, 7, 11204
Mo_2C/NCF	0.28	0.5 M H_2SO_4	40	144	55	ACS Nano. 2016, 10, 11337
2D-N,Co-Mo_2C	0.55	0.1 M $HClO_4$	25	71	40	Adv. Funct. Mater. 2017, 1703933.
Co-Mo_2C-0.020	0.14	0.5 M H_2SO_4	40	140	39	Adv. Funct. Mater. 2016, 26, 5590.
Mo_2C/RGO	0.285	0.5 M H_2SO_4	70	130	57.3	Chem. Commun. 2014, 50, 13135.
Mo_2C/CNT-GR	0.65	0.5 M H_2SO_4	62	130	58	ACS Nano 2014, 8, 5164.
Mo_2C@NC	0.28	0.5 M H_2SO_4	---	124	60	Angew. Chem. Int. Ed. 2015, 54, 10752
Mo_2C nanotubes	0.75	0.5 M H_2SO_4	82	172	62	Angew. Chem. Int. Ed. 2015, 54, 15395.
np-Mo_2C NWs	0.21	0.5 M H_2SO_4	70	130	53	Energy Environ. Sci. 2014, 7, 387
Mo_2C/CNT	2.0	0.1 M $HClO_4$	---	152	65	Energy Environ. Sci. 2013, 6, 943.
Fe_3C-GNRs	---	0.5 M H_2SO_4	32	49	46	ACS Nano 2015, 9, 7407.
Fe_3C-Mo_2C/NC	0.14	0.5 M H_2SO_4	42	116	43	ChemSusChem 2017, 10, 2597.
Fe_3C/Mo_2C@NPGC	0.14	0.5 M H_2SO_4	18	98	45.2	J. Mater. Chem. A 2016, 4, 1202.
VC-NS	0.28	0.5 M H_2SO_4	---	98	56	Nano Energy 2016, 26, 603.
2D TaC-RGO	0.64	0.5 M H_2SO_4	19	167	58	Chem. Commun. 2016, 52, 8810.
NbC100	---	0.1 M H_2SO_4	>100	470	35	ACS Appl. Mat. Interfaces 2017, 9, 30872.

HER, H_2 evolution reaction; Pt–C, 20 wt% Pt on carbon lack from Johnson–Matthey; RHE, reversible hydrogen electrode.